

A Bayesian search to find high-mass black holes in LIGO data

Author list TBD

(Dated: September 14, 2020)

Abstract

The detection of high mass black holes ($> 100 M_{\odot}$) will shed light on the formation of supermassive black holes and thus galaxy formation. Although LIGO is sensitive to the merger of binary black holes with total masses up to $500 M_{\odot}$, the largest total mass detected so far is approximately $80 M_{\odot}$. A possible explanation for the absence of high mass events may be due to their misclassification as short-duration instrumental noise transients. Short-duration instrumental transients mimic the short-duration gravitational-wave signals from high-mass binary black hole mergers. Here we demonstrate that a new search method utilising Bayesian inference could be a more sensitive tool for detecting high-mass binary black hole mergers as compared to traditional match-filtering. We have applied this technique on the high-mass triggers during LIGO's second observing run to investigate the possibility of discovering new gravitational-wave signals from an entirely new class of high mass black hole binaries. [RS: add sentence describing if we see any new events; add a sentence on our analysis of IAS events]

I. INTRODUCTION

[AV: Need to edit in light of S190521G paper] Since the 1970s, there has been an accumulation of evidence for stellar-mass and supermassive black holes. In 2019, the Event Horizon Telescope provided the first visual evidence of the supermassive black hole M87 [1]. As of January 2020, LIGO, Virgo and IAS [RS: we should think carefully about how to describe the IAS events here; I think our conclusion is that they're not real] have confirmed more than a dozen binary black hole systems [2–6]. These various discoveries have firmly established the existence of stellar-mass black holes, supermassive black holes and binary black hole systems. Interestingly, there is still no direct evidence for intermediate-mass black holes, the black holes that lie in between stellar-mass and supermassive black hole systems with masses between $10^2 - 10^6 M_\odot$. Thus, the existence of intermediate-mass black holes is still speculative.

If intermediate-mass black holes are present, the gravitational waves emitted from the merger of a binary black hole system with at least one intermediate-mass black hole (up to a mass of $400 M_\odot$) will be detectable by the ground-based gravitational-wave network. Gravitational waves from such systems should occur at a rate of $0 - 10 \text{ yr}^{-1}$ [7–9]. However, even after conducting a targeted matched-filter based search for gravitational waves from intermediate-mass black holes the largest total mass detected so far is approximately $80 M_\odot$ [10–12]. A possible explanation for the absence of intermediate-mass events may be due to their misclassification as short-duration instrumental noise transients known as glitches [13–19]. These glitches can mimic astrophysical signals and hence decrease the significance of true gravitational wave events.

One method to account for glitches while searching for gravitational waves from coalescing compact binaries is by utilising an astrophysical Bayesian odds [20–24]. A true Bayesian odds calculated without using bootstrap techniques can provide events with a more accurate significance that is agnostic to a specific search strategy [22–24]. Additionally, a Bayesian odds can include more information than is included in current matched filter searches such as if the gravitational wave event’s signal is coherent amongst the network of detectors, if the binary system that created the gravitational waves was precessing, and if

the gravitational wave signal contains higher-order modes. It is because Bayesian methods can incorporate all this physical information about a gravitational wave signal that the LIGO Scientific Collaboration uses these methods to determine the source parameters of gravitational wave events [12, 25]. This paper demonstrates that the power of Bayesian methods used in parameter estimation can also successfully be used to discriminate between coherent gravitational-wave signals, incoherent glitches, and Gaussian noise in the form of a Bayesian search.

In this paper we utilise a Bayesian method, called the BCR [21], to search for the significant gravitational wave signals from high-mass (systems with total masses in the range of $55 - 500 M_{\odot}$) compact binary coalescences in the detector data recorded during aLIGO’s second observing run (O2). We find that (a) our search does not identify any unreported stellar mass or intermediate mass black holes; (b) high-mass events reported in the GWTC-1, including GW170729 (an event with disputed p_{astro} amongst various search pipelines) have high low significance; and that (c) high-mass events detected from some independent groups have low significance. [RS: explicitly state that they’re the IAS events]

The remainder of this paper is structured as follows. We outline our methods, including details of the BCR and the retrieval of our candidate events in Section II. We present details on the implementation of our analysis in Section III. Finally we present our results in Section IV, and discuss these results in the context of the significance of gravitational wave candidates in Section V.

II. METHOD

[RS: I think you need a synopsis of this section before going into the details; explain that one could in principle apply bayesian methods only, but we don’t do that here. Instead, we take triggers from pycbc and use bayesian evidences as a ranking statistic etc...]

A. Triggers for Analysis

The LIGO Scientific collaboration runs a number of search pipelines that target gravitational waves from compact binary mergers such as the GstLAL, MBTA, SPIIR and PyCBC searches [12].

At its core, the PyCBC [26] search performs a matched-filter search for binary merger signals by comparing the data against templates from a gravitational-wave template-bank [27]. ~~PyCBC calculates the matched-filter for several different coalescence times and uses numerous templates from the template bank for each section of data being analysed.~~ The output of PyCBC’s search is a signal-to-noise ratio ρ like statistic, called the PyCBC ranking statistic ρ_{PC} . This statistic is a function of the matched-filter ρ , signal-based veto values, intrinsic and extrinsic properties of the apparent signal and other information [27]. Whenever a local maximum of $\rho_{\text{PC}} > \rho_{\text{T}}$, where ρ_{T} is some threshold value, the search pipeline produces a single-detector trigger associated with the detector and time where the data was obtained.

For PyCBC to consider a trigger to be a **candidate trigger**, a trigger from astrophysical origins, the trigger must be observed between detectors with the same template and a time of arrival difference less than the gravitational-wave travel time between detectors [27]. To test its search, PyCBC also conducts searches for **simulated triggers**, artificial triggers manufactured by injecting signals into the detector data. These simulated signal studies provides PyCBC with metrics on its search’s sensitivity. Finally, to quantify the statistical significance of candidate events, PyCBC artificially constructs a **background trigger** set to compare the candidate events against. These background triggers are signal-free events **[RS: not quite: they contain signals, just not coherent ones]**, constructed by applying relative offsets, or time-shifts, between the data of different detectors [27]. Note that the time-shifts to generate the background triggers are greater than the gravitational-wave travel time between detectors to ensure that the background triggers are not of astrophysical origins.

In our work, we demonstrate that the BCR can be used in a similar way as ρ_{PC} , as a ranking statistic, to measure the statistical significance of candidate triggers. Before we

discuss how we use the BCR as a measure of significance, we introduce the method to calculate the BCR in the following section.

B. The Bayesian Coherence Ratio

Bayes theorem states that the probability $P(\mathcal{H}|d)$ for a hypothesis \mathcal{H} and data d is

$$P(\mathcal{H}|d) = \frac{\mathcal{L}(d|\mathcal{H})\pi(\mathcal{H})}{Z} , \quad (1)$$

[RS: see comments from last week on replacing L with Z etc...] where $\mathcal{L}(d|\mathcal{H})$ is the likelihood of the data given the hypothesis, $\pi(\mathcal{H})$ is the prior probability of the hypothesis, and finally, $Z = \sum \mathcal{L}(d|\mathcal{H})\pi(\mathcal{H})$ is the marginalised likelihood called the evidence [AV: Rory suggested we use $Z(d|H)$ instead of $L(D|H)$]. To compare two hypotheses \mathcal{H}_A and \mathcal{H}_B with the Bayes theorem one can calculate an odds ratio

$$\mathcal{O}_B^A = \frac{Z^A \pi(\mathcal{H}_A)}{Z^B \pi(\mathcal{H}_B)} , \quad (2)$$

where Z^A and Z^B are the evidences for the \mathcal{H}_A and \mathcal{H}_B hypotheses. The odds ratio can tell us which of the two hypotheses is more likely. For example, if $\mathcal{O}_B^A \gg 1$, then this odds ratio indicates that the \mathcal{H}_A is much more likely than \mathcal{H}_B .

The BCR is a Bayesian odds ratio like the above, of a coherent signal hypotheses \mathcal{H}_S and an incoherent instrumental feature hypothesis \mathcal{H}_I for a network of D detectors. \mathcal{H}_I states that each detector i has either pure Gaussian noise \mathcal{H}_N or a glitch \mathcal{H}_G . Following Isi et al. [21], the BCR is given by

$$\text{BCR} = \frac{\alpha Z^S}{\prod_{i=1}^D [\beta Z_i^G + (1 - \beta) Z_i^N]} , \quad (3)$$

where Z^S , Z_i^G and Z_i^N are the Bayesian evidences (marginalised likelihoods) for \mathcal{H}_S , \mathcal{H}_N , and \mathcal{H}_G . α and β , are the prior odds for obtaining a signal $\alpha = P(\mathcal{H}_S)/P(\mathcal{H}_I)$ and the prior odds for obtaining a glitch $\beta = P(\mathcal{H}_G)/P(\mathcal{H}_I)$. As the rate of signal and glitches are unknown, these priors α and β are tuned to maximise the BCR distributions for background data (signal-free data) and simulated signals [21].

C. Bayesian Evidence Evaluation

1. Noise Model

We assume that each detector's noise is Gaussian and stationary over the period being analysed [28]. In practice, we estimate the noise variance using the noise power spectral density (PSD) σ_i^2 of the data. [RS: NOTE: σ_i^2 is the noise variance, not the PSD. If you compare the likelihood in, e.g., veitch and vecchio to yours you can see how to relate the variance to the PSD and vice versa]. Using the σ_i^2 , for each data segment d_i in each of the i detectors in a network of D detectors, we can write

$$Z_i^N = \mathcal{N}(d_i) = \frac{1}{2\pi\sigma_i^2} \exp\left(-\frac{1}{2} \frac{d_i^2}{\sigma_i^2}\right), \quad (4)$$

where $\mathcal{N}(d_i)$ is a normal distribution with a mean of zero and variance proportional to the σ_i^2 .

2. Coherent Signal Model

We model coherent signal using a binary black hole waveform template $\mu(\vec{\theta})$, where the vector $\vec{\theta}$ contains a point in the 15 dimensional space describing precessing binary-black hole mergers. For the signal to be coherent, $\vec{\theta}$ must be consistent in each 4 s data segment d_i for a network of D detectors, Hence, the coherent signal evidence is calculated as

$$Z^S = \int_{\vec{\theta}} \prod_{i=1}^D \left[\mathcal{L}(d_i | \mu(\vec{\theta})) \right] \pi(\vec{\theta} | \mathcal{H}_S) d\vec{\theta}, \quad (5)$$

where $\pi(\theta | \mathcal{H}_S)$ is the prior for the parameters in the coherent signal hypothesis, and $\mathcal{L}(d_i | \mu(\vec{\theta}))$ is the likelihood for the coherent signal hypothesis that depends on the gravitational wave template $\mu(\vec{\theta})$ and its parameters $\vec{\theta}$.

3. Incoherent Glitch Model

Finally, as glitches are challenging to model and poorly understood, we utilise a surrogate model for glitches: the glitches are modelled using gravitational wave templates $\mu(\vec{\theta})$ with uncorrelated parameters amongst the different detectors such that $\vec{\theta}_i \neq \vec{\theta}_j$ for two detectors

i and j [20]. Modelling glitches with $\mu(\vec{\theta})$ captures the worst case scenario: when glitches appear similar to gravitational wave signals. Thus, we can write Z_i^G as

$$Z_i^G = \int_{\vec{\theta}} \mathcal{L}(d_i|\mu(\vec{\theta})) \pi(\vec{\theta}|\mathcal{H}_G) d\vec{\theta}, \quad (6)$$

where $\pi(\theta|\mathcal{H}_G)$ is the prior for the parameters in the incoherent glitch hypothesis.

D. Tuning the BCR

After calculating the BCR for a set of background triggers and simulated triggers from a stretch of detector-data, we can compute probability distributions for the background and simulated triggers, $p_b(\text{BCR})$ and $p_s(\text{BCR})$. We expect the background trigger and simulated signal BCR values to favour the incoherent glitch and the coherent signal hypothesis, respectively. Ideally these distributions that represent two unique populations should be distinctly separate and have no overlap in their BCR values. The prior odds parameters α and β from Eq. 3 help separate the two distributions. Altering α translates the BCR probability distributions while adjusting β spreads the distributions. Although Bayesian hyper-parameter estimation can determine the optimal values for these parameters, an easier approach is to manually adjust the parameters for each data chunk's [RS: have you introduced the idea of the pycbc chunk yet?] BCR distribution. In this study, we manually tune α and β to maximally separate the BCR distributions for the background and simulated triggers.

To calculate the separation between $p_b(\text{BCR})$ and $p_s(\text{BCR})$, we use the Kullback–Leibler divergence (KL divergence) D_{KL} , given by

$$D_{KL}(p_b|p_s) = \sum_{i=1}^N p_b(\text{BCR}_i) \cdot (\log p_b(\text{BCR}_i) - \log p_s(\text{BCR}_i)). \quad (7)$$

The $D_{KL} = 0$ when the distributions are identical and increases as the asymmetry between the distributions increases.

We limit our search for the maximum KL-divergence in the α and β ranges of $[E-10, E0]$ as values outside this range are nonphysical. We set our values for α and β to those which

provide the highest KL-divergence and can now calculate the BCR for candidate events present in this stretch of detector-data. Note that we conduct the analysis in stretches of data rather than an entire data set as the background may be different at different points of the entire data set.

E. Calculating the Significance of Candidate events

With the tuned values of α and β we can calculate the BCR for candidate events. As mentioned previously, irrespective of the BCR's Bayesian interpretation, we treat the BCR as a traditional detection statistic to obtain a frequentist estimate of the significance of candidate event measured against the background of signal-free data.

We expect the background trigger BCR values to favour the incoherent glitch hypothesis (the null hypothesis). Candidate event BCR values will either be statistically insignificant compared to the background triggers, implying the candidate is a glitch, or statistically significant to the background distribution, indicating the possible presence of an astrophysical signal. To quantify the level of significance we can calculate a p -values for the candidate events. Here, the p -value tells us how probable it is for the candidate event to be a glitch. Hence, we can use the p -value to calculate

$$p_{\text{astro}} = 1 - p\text{-value} , \quad (8)$$

where p_{ASTRO} is the probability that a signal is of astrophysical origin [29–31].

III. ANALYSIS

A. Acquisition of triggers

Advanced LIGO's second observing run O2 lasted 38 weeks [32]. The software package, PyCBC [26], processed the O2 data in 22 time-frames (approximately 2 weeks for one time-frames) and found several gravitational wave events and numerous gravitational wave candidates [33–38]. Some candidate events were vetoed to be glitches, while others due to their low significance. The data is divided into these time-frames because the detector's

TABLE I: Template Banks's parameters for templates with duration < 454 ms.

	Minimum	Maximum
Component Mass 1 [M_{\odot}]	31.54	491.68
Component Mass 2 [M_{\odot}]	1.32	121.01
Total Mass [M_{\odot}]	56.93	496.72
Chirp Mass [M_{\odot}]	8.00	174.56
Mass Ratio	0.01	0.98

sensitivity does not stay constant throughout 8 month long observing period.

In addition to finding candidate events, `PyCBC` also manufactured several million background triggers for each time-frames, to quantify the significance of the candidate events when compared to the background for the respective time-frames. Finally, to test the search's sensitivity, `PyCBC` simulated and searched for thousands of artificial signals.

For our study, we filter the background, simulated and candidate events to include only high-mass events with masses in the ranges of the parameters presented in Table~I. A plot of the `PyCBC` triggers from one time-frame, during April 23 - May 8, 2017, is presented in Figure 1. This figure also depicts the gravitational wave templates used during the search through this time-frame of data.

B. Calculating the BCR for triggers

To evaluate Z^S , Z_i^G and Z_i^N as shown in Eqs. 4-6 and calculate the BCR Eq. 3 for these triggers, we carry out Bayesian inference with `BILBY` [39], employing `DYNesty` [40] as our nested sampler. Nested sampling, an algorithm introduced by [?], provides an estimate of the true Bayesian evidence and is often utilised for parameter estimation within the LIGO collaboration [39].

The most computationally intensive step during Bayesian inference is the evaluation of

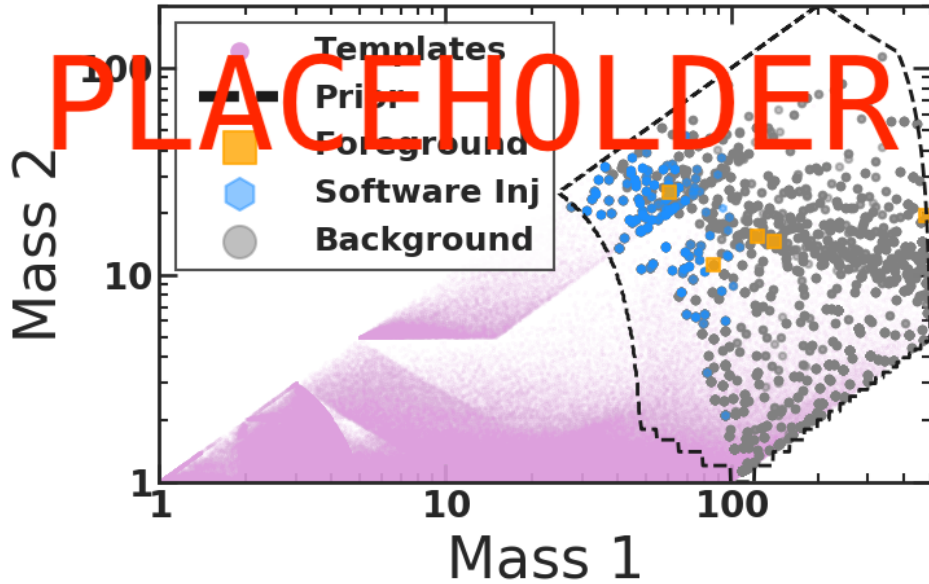


FIG. 1: The template bank used by PyCBC to search a section of O2 data from April 23 - May 8, 2017. Our search is constrained to the high-mass parameter space enclosed by the dashed line.

the likelihood $\mathcal{L}(d_i|\mu(\vec{\theta}))$. To accelerate our analysis, we use a likelihood that explicitly marginalises over coalescence time, phase at coalescence, and luminosity distance (Eq. 80 from Thrane and Talbot [41]). While this marginalised likelihood reduces the run time without introducing errors to our evidence evaluation, it does not generate samples for the marginalised parameters. However, these parameter samples can be calculated as a post-processing step [41].

We set the priors $\pi(\vec{\theta}|\mathcal{H}_S)$ and $\pi(\vec{\theta}|\mathcal{H}_G)$ to be identical. These priors restrict signals with mass parameters in the ranges presented in Table~I. The spins are aligned over a uniform range for the dimensionless spin magnitude from $[0, 1]$. The luminosity distance prior assigns probability uniformly in comoving volume, with an upper cutoff of 5 Gpc. The remaining priors are the same as the those used for in GWTC-1.

The waveform template we utilise is IMRPHENOMPv2, a phenomenological waveform template constructed in the frequency domain that models the in-spiral, merger, and ring-down (IMR) of a compact binary coalescence [42]. Although gravitational wave templates such as SEOBNRv4PHM [?] created from numerical relativity simulations incorporate

more physics such as information on higher-order modes, we still use IMRPHENOMPv2 as it evaluates faster than numerical relativity models [RS: NOTE: SOEOB is not a NR waveform. It’s just tuned to NR].

To generate the PSD σ_i^2 [RS: see comment about difference between the psd and the noise variance], we take 31 neighbouring, off-source, non-overlapping, 4 s segments of time-series data prior to the data segment d_i being analysed. A Tukey window with a roll off of 0.2 s is applied to each data segment to suppress spectral leakage after which the segments are fast-Fourier transformed and median-averaged to create a σ_i^2 [28]. This method, like other σ_i^2 estimation methods, adds statistical uncertainties to the σ_i^2 [43]. To marginalise over the statistical uncertainty we use the median-likelihood presented by Talbot and Thrane [43] as a post-processing step and shift our Bayesian Evidence estimations closer to their true astrophysical values.

Finally, we neglect detector calibration uncertainty and acquire data from the Gravitational Wave Open Science Center [32]. The data we use is the publicly accessible O2 strain data from the Hanford and Livingston detectors. To ensure the data is usable we verify that the analysis and PSD data are obtained when the detectors are in “Science Mode”. The data requisition and quality checks are conducted using `GWPY` [?].

The run-time to calculate a single Bayesian evidence after using `DYNesty` with 1,000 live points and 100 walkers is usually between 0.5 – 12 hours (where the run time often depends on the SNR of the data segment).

C. Assigning p_{astro} to candidate events

After the calculating the BCR for the entire set of high-mass background and simulated triggers, we calculate probability distributions $p_b(\text{BCR})$ and $p_s(\text{BCR})$ for each 2-week time-frame of O2 data. These distributions are used to obtain the “tuned” prior-odd α and β values that maximise $D_{KL}(p_b|p_s)$ for each time-frame of data.

Finally, using the tuned prior odds the BCR for the candidate events can be calculated. Figure 2 shows the BCR distributions for the background triggers, simulated triggers and candidate events. The bulk of the background and simulated trigger distributions are separate but have a slight overlap due to some of the simulated signal's being very faint [AV: but the BCR should still be able to find the injections and set them to have high BCRs? Could it be that the signals are injected over sketchy-glitch like data? How can I verify this?] [RS: you expect that some genuine signals will be reported as a glitch or noise, e.g., an odds of 1/10 means that you expect that 1 time out of ten a signal is mis classified a noise, and vice versa. You can get a signal at any bayes factor]. This suggests that the BCR can successfully distinguish signals from noise or glitches. The vertical lines in Figure 2 displays the BCR for gravitational wave candidate events. On comparing the candidate event BCR values with the background distribution, we can estimate p_{astro} values for the candidate events.

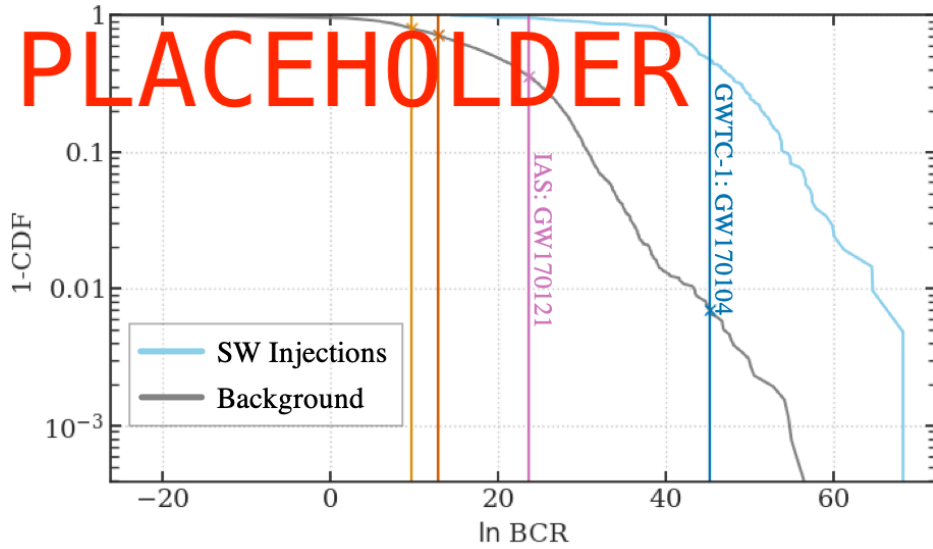


FIG. 2: Histograms represent the survival function (1-CDF) from our selection of $\sim 3,000$ background triggers (grey) and 648 simulated signals (blue) triggers obtained from PyCBC's search of data from April 23 - May 8, 2017. Vertical lines mark the ln BCRs of two glitches (orange and yellow), IAS's GW170121 (pink), and GWTC-1's GW170104 (dark blue).

TABLE II: p_{astro} from several detection pipelines for a subset of the O2 foreground triggers.

Event	Catalogue	PyCBC	GstLAL	cWB	IAS	BCR
GW170104	GWTC-1	1	1	1	0.99	0.99
GW170121	IAS-1	NA	NA	NA	0.99	0.65
GWC170402	IAS-2	NA	0.086	NA	0.68	0.33
GW170403	IAS-1	NA	NA	NA	0.56	0.33
IMBHC170423	IMBH-marginal	NA	0.95	1	NA	0.01
GW170425	IAS-1	NA	NA	NA	0.77	0.36
GW170502	Udall et al.	NA	NA	NA	NA	0.40
GW170729	GWTC-1	0.52	0.98	0.94	NA	0.98

IV. RESULTS

[AV: I should use Pratten et al's table + values here] In aLIGO's first two observing runs, eleven gravitational wave events were found in the data by the LIGO-Virgo scientific collaboration [12]. Since the public release of LIGO's first and second observing run's data, several groups have searched the data for gravitational waves independently of LIGO. One particular research group of interest is a research team at the Institute for Advanced Study (IAS). The group constructed searches to look for the LIGO-confirmed the gravitational wave events detected by the LIGO-Virgo collaboration, and in the process of doing so, claim to have discovered several others events [3–5]. Some of these events have total masses $> 85 M_{\odot}$, which is larger than the average total mass of the LIGO detections. Some of these IAS and LIGO events are displayed in Table~II with their p_{astro} reported by various LIGO and IAS search pipelines.

From this Table~II, it is evident there is some uncertainty if these events can be considered real gravitational-wave events – are these events significantly different from the background or not? The various pipelines have different answers. Our BCR p_{astro} shows support that the LIGO-VIRGO events come from an astrophysical source, while the candidate events from the IAS group appear to have a lower probability of originating from an astrophysical source.

V. CONCLUSION

[RS: lead with something specific to your work; what did you find/learn? how can it be extended? what does it imply for high mass BBH? How do the reported BCRs on interesting events compare to other bayesian measures of significance/odds? etc...It might be useful to take a look at some of the pycbc search papers for how to summarize results from a search]The detection of high mass black holes $> 100 M_{\odot}$ will shed light on the formation of globular clusters, supermassive black holes and thus galaxy formation [44, 45]. LIGO is theoretically sensitive to the merger of binary black holes with total masses up to $500 M_{\odot}$ which are expected to occur at a rate of $0-10 \text{ yr}^{-1}$ [7, 8]. However, even after Abbott et al. [11]’s targeted match-filter based search for gravitational waves from high-mass black holes the largest total mass detected so far is approximately $80 M_{\odot}$ [12]. A possible explanation for the absence of high mass events may be due to their misclassification as short-duration instrumental noise transients [?]. High-mass mergers have very few in-band wave cycles, and hence can easily be mistaken for short-duration instrumental transients.

We have developing a targeted search for gravitational waves from high-mass black hole systems. This targeted search utilises Bayesian inference and provides a ranking statistic that contains a lot of physical information about the high-mass systems. We have applied this technique on all the high-mass triggers identified by PYCBC during LIGO’s second observing run to investigate the possibility of discovering new gravitational-wave signals from high mass black hole binaries. Although we were unable to uncover new gravitational waves events, we were able to report high p_{astro} for events already detected by LIGO, and low p_{astro} for some events identified by external pipelines.

Acknowledgments

This research has made use of data, software and/or web tools obtained from the Gravitational Wave Open Science Center (<https://www.gw-openscience.org>), a service of LIGO Laboratory, the LIGO Scientific Collaboration and the Virgo Collaboration. LIGO is funded by the U.S. National Science Foundation. Virgo is funded by the French Centre National de Recherche Scientifique (CNRS), the Italian Istituto Nazionale della Fisica Nucleare (INFN)

and the Dutch Nikhef, with contributions by Polish and Hungarian institutes.

- [1] Event Horizon Telescope Collaboration, K. Akiyama, A. Alberdi, W. Alef, K. Asada, R. Azulay, A.-K. Baczko, D. Ball, M. Baloković, J. Barrett, et al., *ApJ* **875**, L4 (2019), 1906.11241.
- [2] B. P. Abbott, R. Abbott, T. D. Abbott, et al. (LIGO Scientific Collaboration and Virgo Collaboration), *Phys. Rev. X* **9**, 031040 (2019), URL <https://link.aps.org/doi/10.1103/PhysRevX.9.031040>.
- [3] T. Venumadhav, B. Zackay, J. Roulet, L. Dai, and M. Zaldarriaga, *Physical Review D* **100**, 023011 (2019).
- [4] T. Venumadhav, B. Zackay, J. Roulet, L. Dai, and M. Zaldarriaga, arXiv e-prints arXiv:1904.07214 (2019), 1904.07214.
- [5] B. Zackay, L. Dai, T. Venumadhav, J. Roulet, and M. Zaldarriaga, arXiv e-prints arXiv:1910.09528 (2019), 1910.09528.
- [6] A. H. Nitz, T. Dent, G. S. Davies, S. Kumar, C. D. Capano, I. Harry, S. Mozzon, L. Nuttall, A. Lundgren, and M. Tápai, *ApJ* **891**, 123 (2020), 1910.05331.
- [7] J. M. Fregeau, S. L. Larson, M. C. Miller, R. O’Shaughnessy, and F. A. Rasio, *The Astrophysical Journal Letters* **646**, L135 (2006), URL <https://iopscience.iop.org/article/10.1086/507106/pdf>.
- [8] I. Mandel, D. A. Brown, J. R. Gair, and M. C. Miller, *The Astrophysical Journal* **681**, 1431 (2008), URL <http://www.chgk.info/~ilyamandel/papers/mbgm2008.pdf>.
- [9] C. L. Rodriguez, M. Morscher, B. Pattabiraman, S. Chatterjee, C.-J. Haster, and F. A. Rasio, *Physical Review Letters* **115**, 051101 (2015), URL <https://journals.aps.org/prl/pdf/10.1103/PhysRevLett.115.051101>.
- [10] J. Aasi, B. Abbott, R. Abbott, T. Abbott, M. Abernathy, T. Accadia, F. Acernese, K. Ackley, C. Adams, T. Adams, et al., *Physical Review D* **89**, 122003 (2014), URL <https://arxiv.org/abs/1404.2199>.
- [11] B. P. Abbott, R. Abbott, T. D. Abbott, et al. (LIGO Scientific Collaboration and Virgo Collaboration), arXiv e-prints arXiv:1906.08000 (2019), 1906.08000.
- [12] B. Abbott, R. Abbott, T. Abbott, S. Abraham, F. Acernese, K. Ackley, C. Adams, R. Adhikari, V. Adya, C. Affeldt, et al., *Physical Review X* **9**, 031040 (2019), URL <https://arxiv.org/>

pdf/1811.12907.pdf.

- [13] L. Blackburn, L. Cadonati, S. Caride, S. Caudill, S. Chatterji, N. Christensen, J. Dalrymple, S. Desai, A. Di Credico, G. Ely, et al., Classical and Quantum Gravity **25**, 184004 (2008), 0804.0800.
- [14] N. J. Cornish and T. B. Littenberg, Classical and Quantum Gravity **32**, 135012 (2015), 1410.3835.
- [15] L. K. Nuttall, T. J. Massinger, J. Areeda, J. Betzwieser, S. Dwyer, A. Effler, R. P. Fisher, P. Fritschel, J. S. Kissel, A. P. Lundgren, et al., Classical and Quantum Gravity **32**, 245005 (2015), 1508.07316.
- [16] B. P. Abbott, R. Abbott, T. D. Abbott, M. R. Abernathy, F. Acernese, K. Ackley, M. Adamo, C. Adams, T. Adams, P. Addesso, et al., Classical and Quantum Gravity **33**, 134001 (2016), 1602.03844.
- [17] A. H. Nitz, Classical and Quantum Gravity **35**, 035016 (2018), 1709.08974.
- [18] J. Powell, Classical and Quantum Gravity **35**, 155017 (2018), 1803.11346.
- [19] M. Cabero, A. Lundgren, A. H. Nitz, T. Dent, D. Barker, E. Goetz, J. S. Kissel, L. K. Nuttall, P. Schale, R. Schofield, et al., Classical and Quantum Gravity **36**, 155010 (2019), 1901.05093.
- [20] J. Veitch and A. Vecchio, Phys. Rev. D **81**, 062003 (2010), 0911.3820.
- [21] M. Isi, R. Smith, S. Vitale, T. J. Massinger, J. Kanner, and A. Vajpeyi, Phys. Rev. D **98**, 042007 (2018), 1803.09783.
- [22] G. Ashton, E. Thrane, and R. J. E. Smith, Phys. Rev. D **100**, 123018 (2019), 1909.11872.
- [23] G. Ashton and E. Thrane, MNRAS (2020), 2006.05039.
- [24] G. Pratten and A. Vecchio, arXiv e-prints arXiv:2008.00509 (2020), 2008.00509.
- [25] B. Abbott, S. Jawahar, N. Lockerbie, and K. Tokmakov, PHYSICAL REVIEW D Phys Rev D **93**, 122003 (2016), URL <https://arxiv.org/pdf/1602.03839.pdf>.
- [26] A. Nitz, I. Harry, D. Brown, C. M. Biwer, J. Willis, T. D. Canton, C. Capano, L. Pekowsky, T. Dent, A. R. Williamson, et al., *gwastro/pycbc: Pycbc release 1.16.4* (2020), URL <https://doi.org/10.5281/zenodo.3904502>.
- [27] G. S. Davies, T. Dent, M. Tápai, I. Harry, C. McIsaac, and A. H. Nitz, Phys. Rev. D **102**, 022004 (2020), 2002.08291.
- [28] The LIGO Scientific Collaboration, the Virgo Collaboration, B. P. Abbott, R. Abbott, T. D. Abbott, S. Abraham, F. Acernese, K. Ackley, C. Adams, V. B. Adya, et al., arXiv e-prints

- arXiv:1908.11170 (2019), 1908.11170.
- [29] W. M. Farr, J. R. Gair, I. Mandel, and C. Cutler, *Phys. Rev. D* **91**, 023005 (2015), 1302.5341.
 - [30] S. J. Kapadia, S. Caudill, J. D. E. Creighton, W. M. Farr, G. Mendell, A. Weinstein, K. Cannon, H. Fong, P. Godwin, R. K. L. Lo, et al., *Classical and Quantum Gravity* **37**, 045007 (2020), 1903.06881.
 - [31] S. M. Gaebel, J. Veitch, T. Dent, and W. M. Farr, *MNRAS* **484**, 4008 (2019), 1809.03815.
 - [32] The LIGO Scientific Collaboration, the Virgo Collaboration, R. Abbott, T. D. Abbott, S. Abraham, F. Acernese, K. Ackley, C. Adams, R. X. Adhikari, V. B. Adya, et al., arXiv e-prints arXiv:1912.11716 (2019), 1912.11716.
 - [33] B. Allen, W. G. Anderson, P. R. Brady, D. A. Brown, and J. D. E. Creighton, *Phys. Rev. D* **85**, 122006 (2012), gr-qc/0509116.
 - [34] B. Allen, *Phys. Rev. D* **71**, 062001 (2005), gr-qc/0405045.
 - [35] A. H. Nitz, T. Dent, T. Dal Canton, S. Fairhurst, and D. A. Brown, *ApJ* **849**, 118 (2017), 1705.01513.
 - [36] T. Dal Canton, A. H. Nitz, A. P. Lundgren, A. B. Nielsen, D. A. Brown, T. Dent, I. W. Harry, B. Krishnan, A. J. Miller, K. Wette, et al., *Phys. Rev. D* **90**, 082004 (2014), 1405.6731.
 - [37] S. A. Usman, A. H. Nitz, I. W. Harry, C. M. Biwer, D. A. Brown, M. Cabero, C. D. Capano, T. Dal Canton, T. Dent, S. Fairhurst, et al., *Classical and Quantum Gravity* **33**, 215004 (2016), 1508.02357.
 - [38] A. H. Nitz, T. Dal Canton, D. Davis, and S. Reyes, *Phys. Rev. D* **98**, 024050 (2018), 1805.11174.
 - [39] G. Ashton, M. Hübner, P. Lasky, and C. Talbot, *Bilby: A User-Friendly Bayesian Inference Library* (2019).
 - [40] J. S. Speagle, *MNRAS* **493**, 3132 (2020), 1904.02180.
 - [41] E. Thrane and C. Talbot, *PASA* **36**, e010 (2019), 1809.02293.
 - [42] S. Khan, S. Husa, M. Hannam, F. Ohme, M. Pürrer, X. J. Forteza, and A. Bohé, *Physical Review D* **93**, 044007 (2016), URL <https://arxiv.org/abs/1508.07253>.
 - [43] C. Talbot and E. Thrane, arXiv e-prints arXiv:2006.05292 (2020), 2006.05292.
 - [44] G. Lodato and P. Natarajan, *Monthly Notices of the Royal Astronomical Society* **371**, 1813 (2006).
 - [45] F. Koliopanos, arXiv preprint arXiv:1801.01095 (2018).